Journal of Power Sources 246 (2014) 482–490

Contents lists available at ScienceDirect

Journal of Power Sources

journal homepage: www.elsevier.com/locate/jpowsour

# Improving proton conductivity of sulfonated poly (ether ether ketone) proton exchange membranes at low humidity by semi-interpenetrating polymer networks preparation

Xuemei Wu [a], Gaohong He [a,*], Xiangcun Li [a], Fei Nie [a], Xiaoming Yan [a], Lu Yu [a], Jay Benziger [b,1]

[a] State Key Laboratory of Fine Chemicals, Research and Development Center of Membrane Science and Technology, Dalian University of Technology, Dalian 116024, PR China
[b] Department of Chemical and Biological Engineering, Princeton University, Princeton, NJ 08540, USA

## HIGHLIGHTS

- Proton conductivity at low RH is improved by interpenetrating CrPSSA into SPEEK PEM.
- At RH 25% proton conductivity of SPEEK/CrPSSA 40 reaches $10^{-3}$ S cm$^{-1}$.
- Percolation thresholds of around 0.2 indicate elongated clusters in sIPN membranes.
- It is easy for elongated clusters to swell and interconnect at low RH.
- The sIPN membranes exhibit good miscibility and can be stable up to 250 °C in $N_2$.

## ARTICLE INFO

*Article history:*
Received 21 April 2013
Received in revised form
24 July 2013
Accepted 29 July 2013
Available online 4 August 2013

*Keywords:*
Proton exchange membranes
Interpenetrating polymer networks
Poly (ether ether ketone)
Ionomers
Fuel cells

## ABSTRACT

Crosslinked poly (styrene sulfonic acid) (CrPSSA) is incorporated into sulfonated poly (ether ether ketone) (SPEEK) through the semi-interpenetrating polymer networks (sIPNs) method to improve proton conductivity of SPEEK proton exchange membranes (PEMs) at low relative humidity (RH). Thermogravimetric analysis indicates that the SPEEK/CrPSSA sIPN membrane can be stable up to 250 °C in $N_2$. A single glass transition temperature ($T_g$) of the sIPN measured by differential scanning calorimetric measurements suggests good miscibility of the CrPSSA and SPEEK. At fixed RH the proton conductivity of the sIPN membranes increases as more CrPSSA is incorporated into SPEEK membranes. The sIPN membrane with 40 wt. % CrPSSA has a proton conductivity of $10^{-3}$ S cm$^{-1}$ at 25% RH, which comparable to that of Nafion115 and is 2 orders of magnitude higher than that of the pristine SPEEK membranes ($10^{-5}$ S cm$^{-1}$ at RH 50%). The percolation threshold for proton conduction occurs at lower hydrophilic volume fractions with the increasing content of CrPSSA, suggesting different packing behavior of $-SO_3H$ groups in the SPEEK/CrPSSA sIPN membranes as compared with SPEEK and Nafion® membranes.



## 1. Introduction

Fuel cells (FCs) are electrochemical devices, which convert fuels into electric power with efficient and environmentally friendly way. Among several types of FCs, proton exchange membrane fuel cell (PEMFC) displays advantages of low operating temperature and fast start-up. These advantages make them promising candidates for applications such as automobiles and portable power supplies [1]. A limitation to the applications of PEMFC is the need for the membrane to be humidified in order to have good proton conductivity. It is desirable to operate PEMFC at reduced RH (less than 50%) for the following reasons [2–4]: (1) Decreased water partial pressure at reduced RH results in increased partial pressure of the fuel. This increases the open circuit potential of the fuel cell, which improves electrical power output of PEMFC, especially at temperature higher than 100 °C. (2) Ionomers swell with increased water sorption at high RH which can put stresses on the electrodes and cause electrode failure. (3) At high RH, liquid water accumulates in the porous electrode and flow channels creating mass transport

* Corresponding author. Tel.: +86 411 84707892.
*E-mail addresses:* hgaohong@dlut.edu.cn (G. He), benziger@princeton.edu (J. Benziger).
[1] Tel.: +1 609 258 5416.

0378-7753/$ – see front matter © 2013 Elsevier B.V. All rights reserved.
http://dx.doi.org/10.1016/j.jpowsour.2013.07.108

overpotential losses in the fuel cell. (4) At low RH the fuel cell may be operated with autohumidification so that PEMFC systems can be simplified by getting rid of humidifiers. Despite the advantages of low RH operations in PEMFC, the poor proton conductivity at low RH is a major obstacle to operation at low RH.

Non-fluorinated PEMs are cost-effective membranes that have been suggested as promising candidates for PEMFC [5,6], especially for operating over 100 °C. The mechanical properties of Nafion® deteriorate above 100 °C, especially at low RH. Non-fluorinated PEMs that are based on aromatic heterocyclic polymers with sulfone and carbonyl groups display greater thermal stability ($T_g \sim 300$ °C), as well as lower methanol crossover (methanol permeability $10^{-9}$–$10^{-7}$ $cm^2$ $s^{-1}$) and higher water retention compared with that of Nafion®. Unfortunately the non-fluorinated PEMs have much lower proton conductivity than Nafion® at low relative humidity (RH). Several research groups have shown that non-fluorinated PEMs showed comparable proton conductivity as that of the perfluorinated membranes (e.g. Nafion®) in their fully hydrated state, but show negligible proton conductivity ($<10^{-4}$ S $cm^{-1}$) at RH < 50%, [3,7,8]. In our previous work, we reported much lower proton conductivity of SPEEK membranes ($10^{-5}$ S $cm^{-1}$) as compared to that of Nafion® ($10^{-2}$ S $cm^{-1}$) at RH 50% [9].

Strategies to improve proton conductivity at low RH include inorganic hybrids, non-aqueous solvents and polymer blends. [10] Hydroscopic inorganic nanoparticles ($SiO_2$, $TiO_2$, montmorillonite (MMT) etc.) are incorporated into PEMs to increase water retention at low RH [11,12]. Inorganic solid state protonic conductors (heteropolyacids, super solid acids and Cesium hydrogen sulfate etc.) conduct proton in the absence of water, however their proton conductivity below 100 °C are very low ($10^{-6}$–$10^{-4}$ S $cm^{-1}$) [13,14]. Another approach is to replace water with non-aqueous low volatility solvents, such as $H_3PO_4$, ionic liquids as the proton acceptors [15,16]. The modified PEMs can be operated in anhydrous conditions, but the ionic liquids and non-aqueous solvents are the leached from the membrane by the product water which leads to the decay of the FC performance. Organic proton carriers, such as poly (styrene sulfonic acid) (PSSA), poly (2-acrylamido-2-methyl propane sulfonic acid) (PAMPS), sulfosuccinic acid can increase concentration of $-SO_3H$ by blending or crosslinking with the PEM matrix [17–19]. In the literature, PVA/PSSA blending PEMs were reported to have comparable proton conductivity (around $10^{-3}$ S $cm^{-1}$) as that of Nafion® at low RH (30%). Concerns on this type of PEMs involve in the swelling/conductivity balance and the miscibility of the blending systems.

Over the last decade, (semi) interpenetrating polymer networks ((s)IPNs) have been proposed for applications as PEMs. These properties of the sIPNs can be tailored, including the proton conductivity, mechanical stability, as well as keeping good miscibility of the membranes [20–22]. A recent review summarized the applications of (s)IPNs for PEMFC [23]. IPNs are defined as a combination of two or more polymer networks synthesized in juxtaposition [24], while sIPNs differ from IPNs in that they are composed of one linear polymer entrapped within the network of another polymer. The thermodynamically favored macrophase separation process in most polymer blends can be restricted by rapid quenching of the networks formation during the preparation of (s)IPNs. Microphase separated structure with different shapes and sizes of domains can be obtained [25]. In our previous studies, hydrophilic crosslinked poly (acrylic acid) (CrPAA) network was interpenetrated with sulfonated poly (phthalazinone ether sulfone ketone) (SPPESK) polymer matrix [26–28]. Although water uptake and proton conductivity at the fully hydrated state were enhanced, the carboxyl groups did not improve proton conductivity at low RH.

In this work, a more acidic monomer, sodium 4-styrenesulfonate (NaSS), is used as the interpenetrating monomer to improve the proton conductivity of SPEEK PEMs at low RH. Although linear or crosslinked PSSA has been used as polyelectrolyte in sIPNs architectures, to the best of our knowledge, no efforts have yet dealt with building sIPNs through *in-situ* polymerization/crosslinking of NaSS monomer, as well as detecting percolation threshold for proton conduction in sIPN PEMs. We report here that at low RH proton conductivity of the SPEEK/CrPSSA sIPN membranes gradually increase to the level of Nafion® as NaSS content increased. And the percolation thresholds for proton conduction in the SPEEK/CrPSSA sIPNs PEMs are in between that of Nafion® and the pristine SPEEK membranes. We suggest a packing structure of the hydrophilic domains in the SPEEK/CrPSSA sIPN membranes that can account for the elevated proton conductivity at low RH. To better understand the influence of polymerization/interpenetration of NaSS on the properties of the SPEEK/CrPSSA sIPN membranes, water uptake, swelling strain, as well as thermal stability and miscibility of the sIPN membranes are also investigated in this work.

## 2. Experimental

### 2.1. Materials

PEEK resin was purchased from Professional Plastics, US (VESTAKEEVR 4000G: density 1.30 g $cm^{-3}$, melting temperature 340 °C). Sodium 4-styrenesulfonate (NaSS), divinyl benzene (DVB), benzoyl peroxide (BPO), *N*-methyl-2-pyrrolidone (NMP) and other chemicals were analytical grade and used as received. Nafion115 membrane was obtained from Ion Power.

### 2.2. Preparation of the SPEEK/CrPSSA sIPN membranes

#### 2.2.1. Sulfonation of PEEK

Sulfonation of PEEK was performed according to homogeneous method [9,12]. PEEK (5 g) was dissolved in 100 ml of 95% concentrated sulfuric acid at ambient temperature. The solution was placed in a 60 °C water bath and stirred for 50 min. The reactant was quenched with ice water to precipitate SPEEK. The SPEEK was washed with deionized water until neutral and then dried in vacuum at 80 °C for 24 h.

#### 2.2.2. Preparation of SPEEK/CrPSSA sIPN membranes

The preparation procedure of the SPEEK/CrPSSA sIPN membranes is schematically shown in Fig. 1. Dry SPEEK was dissolved in NMP to form 7 wt. % solution. Monomer NaSS, crosslinker DVB and initiator BPO were dissolved in NMP with a weight ratio of 1:0.15:0.05, and then added to the SPEEK solution. The mixture was stirred and then sealed in a 95 °C oven for 24 h to perform the *in-situ* free radical polymerization/crosslinking of NaSS/DVB. The resulting solution was cast on a glass plate and kept in 40 °C oven for 3 days to evaporate the solvent. A SPEEK membrane was also cast from the 7 wt. % SPEEK solution.

Post treating procedures of the membranes were performed for the purpose of further purification and protonation. Nafion115 was boiled in 3% $H_2O_2$/0.5 M sulfuric acid/deionized water sequentially for 1 h each. While SPEEK and SPEEK/CrPSSA sIPN membranes were boiled in 0.5 M sulfuric acid/deionized water sequentially for 1 h each. Through this procedure, $-SO_3Na$ groups in CrPSSA were converted into $-SO_3H$ groups, and the soluble portion of the sIPN membrane was eliminated. DVB covalently crosslinked the PSSA chains rendering the CrPSSA insoluble; only 10 wt. % of PSSA was not crosslinked and dissolved in boiling water. The resulting protonated membranes were dried in vacuum at 80 °C for 2 days. The drying procedure also annealed the extruded Nafion115 to eliminate thermal history, producing an isotropic Nafion membrane [30]. The dry membrane thicknesses were about 80–100 μm.

In order to determine the composition of the sIPN membranes, the SPEEK/CrPSSA sIPN membrane was soaked in NMP at 90 °C for 5 days

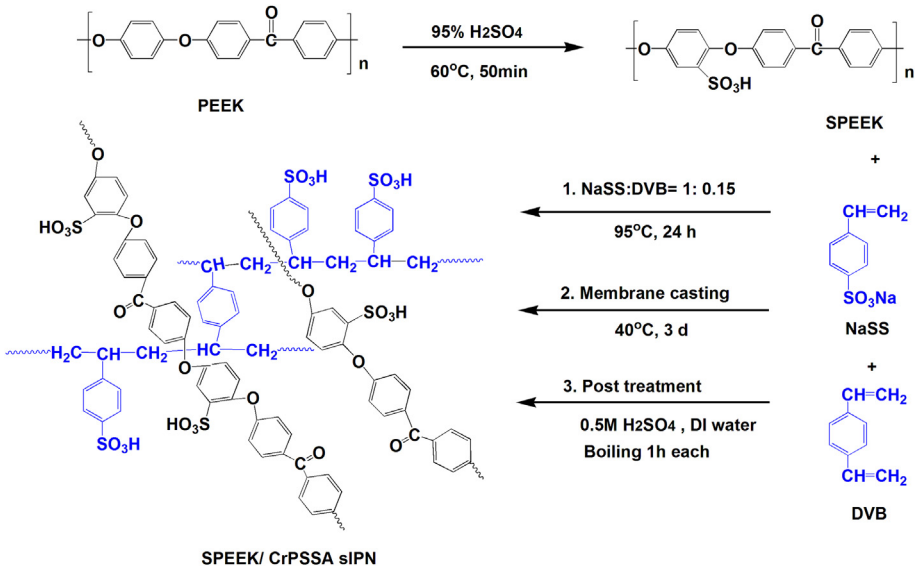


**Fig. 1.** Synthetic schematics of SPEEK/CrPSSA sIPN.

(changing NMP occasionally) to remove the linear SPEEK polymer from the sIPN membranes. The insoluble residue was denoted as extracted CrPSSA. The insoluble residue was washed with deionized water, dried in vacuum at 80 °C for 2 days and then weighed.

### 2.3. Characterization of the SPEEK/CrPSSA sIPN membranes

#### 2.3.1. Ionic exchange capacity

Ionic exchange capacity (IEC) of the membranes was measured by titration. A known weight (approximately 0.1 g) of dry membrane was soaked in 25 ml of 3.0 M NaCl solution and shaken occasionally for 24 h. Then the amount of $H^+$ released to the NaCl solution was detected by titration with 0.01 M NaOH. IEC was calculated by the molar consumption of NaOH divided by the weight of the dry membrane. Equivalent weight (EW) was then calculated as the reciprocal of the IEC value.

#### 2.3.2. FTIR

The Fourier transform infrared (FTIR) spectrum was measured by a Thermo Nicolet Nexus instrument in the range of 4000–500 $cm^{-1}$.

#### 2.3.3. TGA

The thermogravimetric analysis (TGA, TGA/SDTA 851) was carried out to investigate thermal stability of the membranes. Approximately 10 mg dry sample membrane was placed in the sample chamber and programmed from 50 °C to 600 °C at a rate of 10 °C $min^{-1}$ in nitrogen atmosphere.

#### 2.3.4. DSC

Glass transition temperature ($T_g$) of the sIPN membranes was determined by differential scanning calorimetry (DSC, METTER TOLEDO DSC822) at a heating rate of 10 °C $min^{-1}$. Each sample was subjected to a heating/cooling cycle in the range of 25–250 °C, and then heated from 50 °C to 250 °C to obtain reproducible $T_g$ value. The onset temperature of the change of slope in the DSC curve is taken to be as $T_g$.

#### 2.3.5. Equilibrium swelling strain

The linear expansion coefficient of the membranes, $\varepsilon$, was measured as a function of RH at 80 °C in a dynamic creep apparatus [31]. Samples were clamped in an environmental chamber, dried in flowing nitrogen at 80 °C for 2 h, and then humidified nitrogen was supplied to the sample chamber. The change in length was recorded as a function of time. The equilibrium swelling strain is assumed to be achieved when the rate of swelling was less than 0.001 inch $h^{-1}$. The linear expansion coefficient $\varepsilon$ can be calculated by Equation (1).

$$\varepsilon = \frac{l_{wet} - l_{dry}}{l_{dry}} \times 100\% \quad (1)$$

where, $l_{wet}$ and $l_{dry}$ are the lengths of the membrane in equilibrium swollen state and dry state, respectively.

#### 2.3.6. Water uptake and proton conductivity

The equilibrium water uptake and proton conductivity were measured as a function of RH at 80 °C using an isometric system similar to the device previously described in the literature [8,29,32]. A PEM sample was mounted inside a vacuum vessel between two stainless steel clamps. The vessel was placed in an 80 °C oven and evacuated to a base pressure of $10^{-6}$ bar, and then 5–50 μl aliquots of water was injected into the vessel at intervals of 0.5–2 h to allow equilibration with the membrane. The vapor pressure P inside the vessel is equal to the partial pressure of water at the vessel temperature. Therefore, relative humidity of the vessel is given by partial pressure of water divided by the saturation water pressure. The difference between the water in the vapor and the water injected is equal to the moles of water absorbed in the membrane, $M$, as given by Equation (2).

$$M = \frac{V_{water\ injected}}{V_W} - \frac{V_{vessel}P}{RT} \quad (2)$$

where $V_{water\ injected}$, $V_W$ and $V_{vessel}$ are the volume of water injected into the vessel, molar volume of water, 18 $cm^3$ $mol^{-1}$, and the volume of the vessel, respectively. Water uptake of the membrane was equal to the weight of water absorbed in the membrane divided by the weight of the dry membrane.

At the same time as water sorption was measured, in-plane membrane resistance, $R$, was measured at the temperature and RH in the isometric vessel. An AC voltage in the frequency of 1–

$10^5$ Hz was applied across the two stainless steel clamps holding the membrane. Proton conductivity, $\sigma$, was calculated by Equation (3), where $l$ is length of the membrane between the two clamps at the temperature and RH in the environmental chamber and $A$ is the cross-sectional area of the wet membrane. The membrane length at different RH was based on the dry length multiplied by the experimentally determined linear expansion coefficient, assuming isotropic expansion in the membrane.

$$\sigma = \frac{l}{RA} \tag{3}$$

## 3. Results and discussion

### 3.1. Preparation of semi-interpenetrating polymer networks

The FTIR spectra of the SPEEK/CrPSSA sIPN membranes, the pristine SPEEK membrane and the extracted CrPSSA are shown in Fig. 2. Hereinafter, SPEEK/CrPSSA $X$ refers to as the sIPN membrane with NaSS content of $X$ wt. %. The extracted CrPSSA, shows the typical features of PSSA. For example split peaks at 1007.5 $cm^{-1}$ and 1034.5 $cm^{-1}$ are caused by in-plane bending of the sulfonic acid substituted phenyl ring [33], and the peak at 1125.3 $cm^{-1}$ corresponds to asymmetric stretching of the sulfonic acid group [15]. The broad peak at 1655.2 $cm^{-1}$ in the extracted CrPSSA spectrum is probably due to the residue water in the sample. CrPSSA is hygroscopic and readily sorbs water vapor from the atmosphere. The main features of SPEEK spectrum are the peak at 1649.3 $cm^{-1}$ (stretching of carbonyl group), the group of peaks from 1597.2 $cm^{-1}$ to 1471.5 $cm^{-1}$ (stretching of phenyl ring), the peak at 1118.5 $cm^{-1}$ (asymmetric stretching of the sulfonic acid group), and the split peaks at 1002.8 $cm^{-1}$ and 1022.7 $cm^{-1}$ (in-plane bending of the sulfonic acid substituted phenyl ring). The spectra of SPEEK/CrPSSA sIPN membranes show the overlay of SPEEK and CrPSSA; not all the peak intensities of the sIPN are additive; the asymmetric stretching of the sulfonic acid group (peaks at around 1126.1–1128.2 $cm^{-1}$) and in-plane bending of the sulfonic acid substituted phenyl ring (peaks at around 1006.7–1012.5 $cm^{-1}$) are enhanced with the increase of CrPSSA content due to the interpenetration of highly sulfonated CrPSSA. FTIR investigations of the different membranes indicate that in the sIPN membrane CrPSSA forms a solvent insoluble network, while the linear SPEEK still has mobility for structural rearrangement in water.

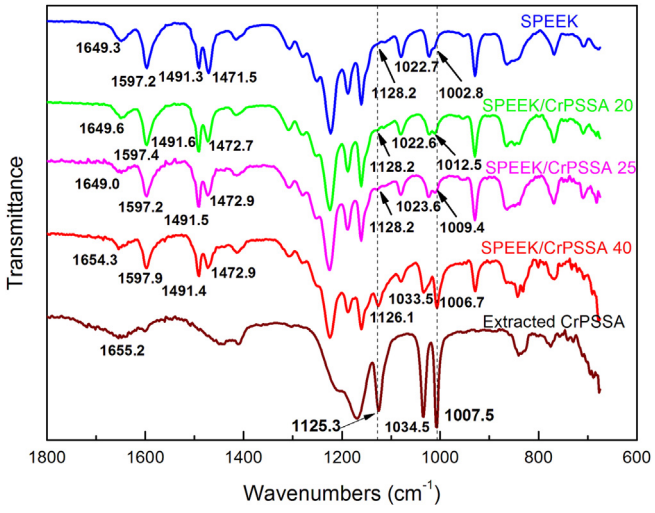


**Fig. 2.** FTIR spectra of SPEEK and SPEEK/CrPSSA sIPN membranes.

Compositions of SPEEK/CrPSSA sIPN membranes prepared in this work are shown in Table 1. All the samples were prepared with fixed weight ratios of NaSS to crosslinker DVB to initiator BPO (1:0.15:0.05). Measured IECs of the samples were in the range of 1.98–2.59, which overlap the range of IEC reported for SPEEK membranes in the literature [34,35]. IECs of the sIPN membranes increased with the increase of NaSS content because of the high IEC of NaSS. Assuming 100% conversion of NaSS and DVB, theoretical IECs of the samples, $IEC_{th}$, could be calculated based on NaSS/DVB content and the IECs of SPEEK and NaSS, as listed in Table 1. The ratio of measured IEC to $IEC_{th}$ can be viewed as an estimate of the minimum conversion of NaSS polymerization/crosslinking in the presence of SPEEK (Since the soluble PASS in the sIPN membranes were eliminated by boiling water before IEC titration). From Table 1, it is seen that the conversion of NaSS in the presence of SPEEK increased with the increase of NaSS content due to the higher concentration of reactant NaSS in the polymerization system. With NaSS content 40%, conversion of NaSS was above 90%.

### 3.2. Thermal stability of the SPEEK/CrPSSA sIPN membranes

Thermal stability of the SPEEK/CrPSSA sIPNs membranes, the pristine SPEEK membrane and the extracted CrPSSA was investigated by TGA. Examples of TGA and their first derivative (DTG) curves are shown in Fig. 3. All membranes exhibit three weight loss steps in the range of 50–600 °C. The first weight loss around 100 °C is related to the evaporation of the absorbed water in the samples. The second weight loss around 250–350 °C is related to desulfonation of the sulfonic acid groups, which coincides with the weight percentage of $-SO_3H$ groups in the membrane calculated by measured IEC (see Table 2). The third weight loss of the SPEEK and SPEEK/CrPSSA sIPN membranes starts from about 470 °C, due to the decomposition of the polymer matrix. While the third weight loss of the extracted CrPSSA starts much earlier (around 340 °C), due to the less thermal stability of CrPSSA main chain [36]. TGA and DTG data indicate that the SPEEK/CrPSSA sIPN membrane only slightly less thermal stability than the pristine SPEEK membrane. It is seen from Table 2 that the onset temperature of desulfonation for SPEEK/CrPSSA sIPN membranes is up to 250 °C in $N_2$, which can meet the requirement for high temperature operation in fuel cells.

### 3.3. Miscibility of the SPEEK/CrPSSA sIPN membranes

Microstructure of PEMs is very important because it has profound effects on the morphology, mechanical, thermal and transport properties of the membranes. Most polymer blends are thermodynamically immiscible, resulting in macrophase separation. Phase separated PEMs may lead to increased fuel crossover, decreased proton conductivity and decreased mechanical stability. Thermodynamic phase separation of sIPNs are kinetically limited

**Table 1**
Compositions of SPEEK/CrPSSA sIPN membranes.

| Samples | NaSS content (wt. %) | EW[a] (g $mol^{-1}$) | IEC (mmeq $g^{-1}$) | $IEC_{th}$[b] (mmeq $g^{-1}$) | Conversion of NaSS (%) |
|---|---|---|---|---|---|
| SPEEK | 0 | 555 | 1.80 | 1.80 | – |
| SPEEK/CrPSSA 20 | 20 | 505 | 1.98 | 2.34 | 84.6 |
| SPEEK/CrPSSA 25 | 25 | 476 | 2.10 | 2.47 | 85.0 |
| SPEEK/CrPSSA 33 | 33 | 418 | 2.39 | 2.67 | 89.5 |
| SPEEK/CrPSSA 40 | 40 | 386 | 2.59 | 2.85 | 90.9 |
| NaSS | 100 | 206 | 4.85 | 4.85 | – |

[a] EW, equivalent weight, refers to as the weight of dry membrane per mole of $-SO_3H$ group.
[b] $IEC_{th} = (100 - X)IEC_{SPEEK} + X \cdot IEC_{NaSS}/(100 + 0.15X)$, where $X$ is the NaSS content, 0.15 is the weight ratio of crosslinker DVB to NaSS.

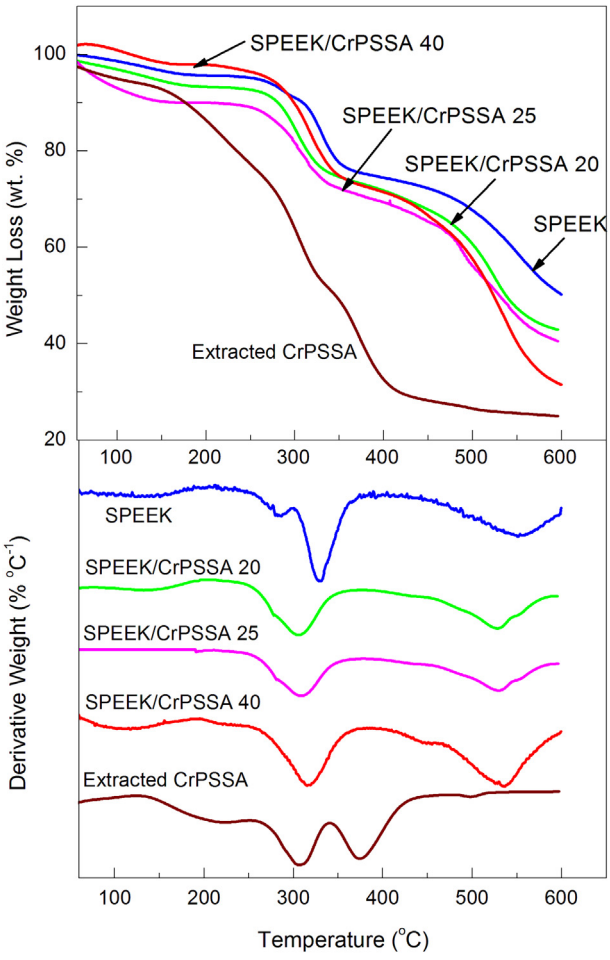


**Fig. 3.** TGA and DTG curves of SPEEK and SPEEK/CrPSSA sIPN membranes.

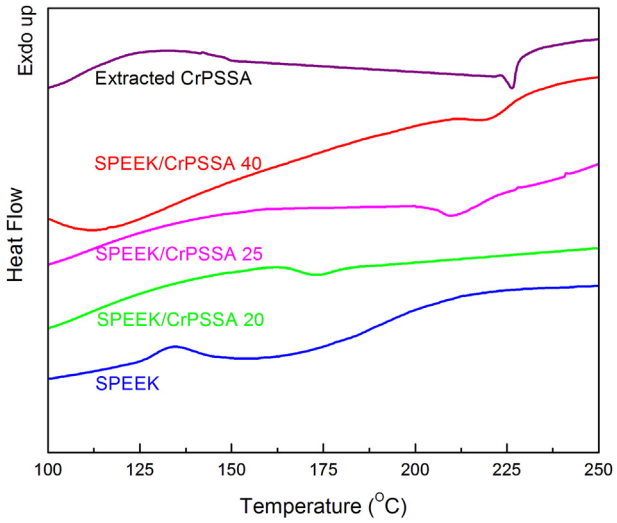


**Fig. 4.** DSC curves of the SPEEK/CrPSSA sIPN membranes.

[20,21]; the degree of phase separation can be controlled by balancing thermodynamically immiscibility and the kinetics of polymer relaxation. The glass transition temperature ($T_g$) can be used to characterize mixing in the sIPN. For a completely phase separated system the glass transitions for each phase should be observed. [37].

Fig. 4 shows the DSC curves detected for SPEEK/CrPSSA sIPN membranes. It can be seen that all SPEEK/CrPSSA sIPN membranes exhibit one single $T_g$ under the testing conditions, which is evidence for good mixing of the two components in the sIPN. $T_g$ values determined by DSC are also listed in Table 2. $T_g$ values of the SPEEK/CrPSSA sIPN membranes are in between that of the SPEEK membrane and the extracted CrPSSA, and increase with the increasing CrPSSA content. It is noticed from Table 2 that the measured $T_g$ values for sIPN membranes are higher than $T_{g,simple}$, the glass transition temperatures calculated according to the simple weight fractional average. The non-linear $T_g$ of the sIPN is indicative of entanglements between different polymer chains restrict mobility of polymer segments. The same results were obtained in the literature and in our previous research on the miscibility of SPPESK/CrPAA sIPN membranes [25,26].

### 3.4. Water sorption and swelling

Water content has great influence on proton conductivity and mechanical stability of PEMs. At low RH, the absorbed water swells the hydrophilic domains and helps to build up continuous hydrophilic pathways for proton transport. While at high RH, too much water may cause excessive swelling of the membranes, resulting in loss of the mechanical strength. In this work, water sorption of the SPEEK, SPEEK/CrPSSA sIPN and Nafion® membranes was investigated as a function of RH, as shown in Fig. 5.

Fig. 5 shows the water content as a function of RH at 80 °C. Water content, when normalized to the number of sulfonic acid groups in Fig. 5 ($\lambda = \#H_2O\,(-SO_3H)^{-1}$), exhibited comparable values for Nafion®, SPEEK and SPEEK/CrPSSA sIPN membranes at low RH (~20%), as was reported in the literature [38]. While at high RH, SPEEK and SPEEK/CrPSSA sIPN membranes exhibited higher values of $\lambda$ than Nafion® membranes; the larger values of $\lambda$ is a typical feature for non-fluorinated PEMs [5–7]. Compared with the pristine SPEEK membrane, SPEEK/CrPSSA sIPN membranes exhibited

**Table 2**
Temperatures of weight losses and glass transition for SPEEK/CrPSSA sIPN membranes.

| Samples | $T_g$ (°C) | $T_{g,\,simple}$[a] (°C) | 2nd weight loss | | | | 3rd weight loss | | | Chart (%) |
|---|---|---|---|---|---|---|---|---|---|---|
| | | | $T_{onset}$ (°C) | $T_{peak}$ (°C) | Loss (wt. %) | | $T_{onset}$ (°C) | $T_{peak}$ (°C) | Loss (wt. %) | |
| | | | | | By TGA | By IEC[b] | | | | |
| SPEEK | 143.7 | – | 256.7 | 333.3 | 19.8 | 14.6 | 486.3 | 555.7 | 25.1 | 50.3 |
| SPEEK/CrPSSA 20 | 169.8 | 160.1 | 250.2 | 310.0 | 19.2 | 16.0 | 468.3 | 532.8 | 24.3 | 44.6 |
| SPEEK/CrPSSA 25 | 204.3 | 164.2 | 253.1 | 319.7 | 16.3 | 17.0 | 476.3 | 526.0 | 29.1 | 40.5 |
| SPEEK/CrPSSA 40 | 215.6 | 176.4 | 257.3 | 322.3 | 23.3 | 21.0 | 475.7 | 540.3 | 41.2 | 31.5 |
| Extracted CrPSSA | 225.5 | – | 252.2 | 302.9 | 27.4 | – | 341.3 | 372.1 | 26.4 | 25.0 |

[a] Calculated by simple wt .% average: $T_{g,simple} = (100 - X)T_{g,SPEEK} + X \cdot T_{g,CrPSSA}/100$, where $X$ is content of NaSS (wt. %) in the sIPN membranes.
[b] The weight percentage of the total $-SO_3H$ groups in the membrane: $(IEC \cdot M_{SO_3H}/1000) \times 100\%$, where $M_{SO_3H}$ is the molar weight of $-SO_3H$ groups, 81 g mol$^{-1}$.

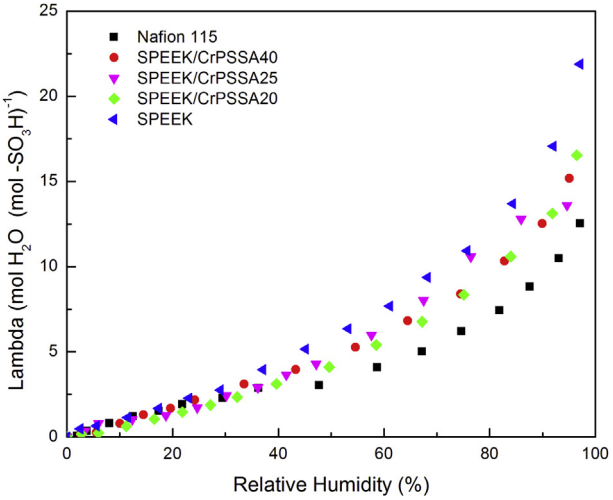


**Fig. 5.** Water content as a function of RH at 80 °C.

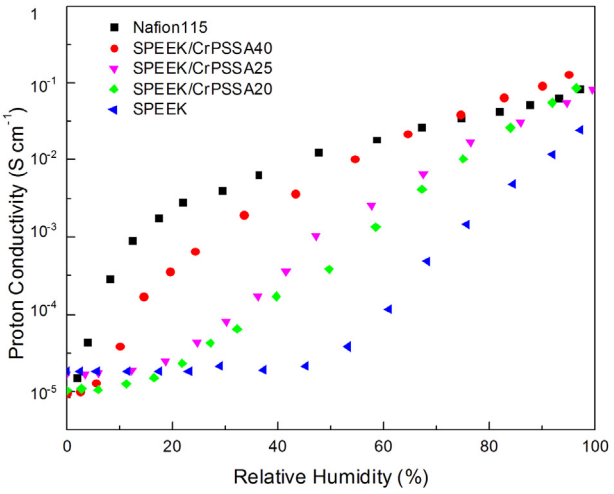


**Fig. 7.** Proton conductivity as a function of RH at 80 °C.

lower values of Lambda, which is due to the higher $-SO_3H$ density of the sIPN membranes.

The linear expansion coefficient of the membranes was measured as a function of RH at 80 °C and shown in Fig. 6. It is seen from Fig. 6 that at high RH SPEEK/CrPSSA sIPN membranes exhibited slightly higher linear expansion coefficients (~18%) than that of Nafion® membrane (12%) because of the higher $-SO_3H$ density in the sIPN membranes. However, at low RH Nafion® showed considerably higher strains. As shown in the amplified graph in the up left of Fig. 6, for RH < 20%, the swelling strains of Nafion® were about 2 times higher than that of the SPEEK membrane. The swelling strains of the SPEEK/CrPSSA sIPN membranes were greater than those for SPEEK and approached that of Nafion® at high RH. It indicates that at low RH Nafion® and the sIPN membranes swelled more than the SPEEK membrane, although all membranes exhibited comparable lambda values (See Fig. 5). Since water swells hydrophilic domains in the PEMs, different water sorption and swelling behaviors at low RH indicate different microstructures of the hydrophilic domains in the membranes, which will be discussed later in Section 3.5.

### 3.5. Proton conductivity at low RH

Proton conductivity of the SPEEK/CrPSSA sIPN membranes as a function of RH at 80 °C is shown in Fig. 7. Data for SPEEK and Nafion115 membranes from our previous work [9] are also plotted in Fig. 7 for comparison. When equilibrated with fully hydrated water vapor, proton conductivity of all the three types of membranes was comparable, reaching values of around $10^{-2}$ S cm$^{-1}$. However, at low RH proton conductivity of the SPEEK membrane was much lower response than that of Nafion®. That is, proton conductivity of the SPEEK membrane was $\leq 2 \times 10^{-5}$ S cm$^{-1}$ until RH 50%, and then increased exponentially to $10^{-2}$ S cm$^{-1}$ at RH 100%. While the proton conductivity of Nafion® reached $10^{-3}$ S cm$^{-1}$ at around RH 15%. Proton conductivities of sIPN membranes were intermediate to SPEEK and Nafion®. For SPEEK/CrPSSA 40 sIPN membrane, proton conductivity increased above $2 \times 10^{-5}$ S cm$^{-1}$ at 10% RH around 10%, which was 100 time less than that of Nafion®. At RH 25%, proton conductivity of SPEEK/CrPSSA 40 sIPN membrane reached $10^{-3}$ S cm$^{-1}$, which was about 80% of the proton conductivity of Nafion® at the same RH. The improved proton conductivity of SPEEK/CrPSSA sIPN membranes at low RH suggests that they may be promising candidates for PEMs applications at low RH and potential alternatives to Nafion® for operations over 100 °C.

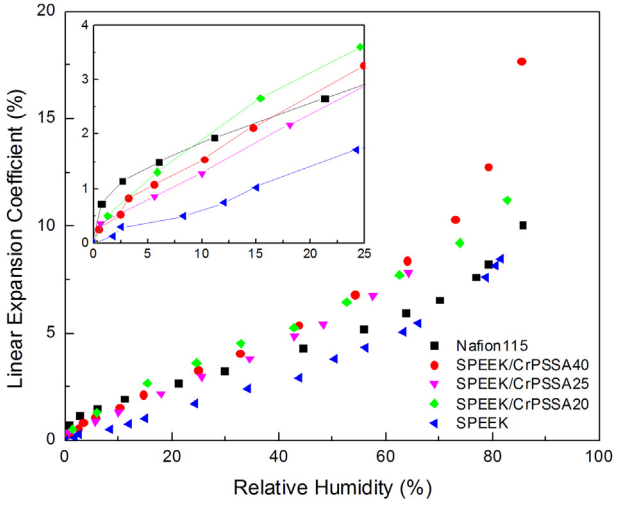


**Fig. 6.** Linear expansion coefficient as a function of RH at 80 °C.

According to the widely accepted ionic cluster model for proton conduction, PEMs possess phase separated morphology, in which the hydrophilic domains form ionic clusters to conduct protons and the hydrophobic polymer main chains provide mechanical and chemical stability of the membranes [39]. Water plays an important role to proton conductivity. The absorbed water swells the hydrophilic domains and establishes continuous pathways for proton transport through the hydrophobic matrix. Following our previous work, the critical hydrophilic volume fraction at which hydrophilic clusters begin to touch each other and form continuous pathways for proton transport is defined as the percolation threshold for proton conduction [9]. And the values of percolation threshold indicate the minimum RH where a PEM will function. According to percolation theory [40], above the percolation threshold, proton conductivity increases as a power law, as shown in Equation (4), where $(\phi_+)_c$ is the percolation threshold, $\phi_+$ is the hydrophilic volume fraction, $\sigma_0$ is the intrinsic conductivity, and the exponent $\alpha$ is an universal constant dependent on the dimensionality of the networks, and for three-dimensional networks $\alpha \approx 2$ [41].

$$\sigma = \sigma_0(\phi_+ - (\phi_+)_c)^{\alpha} \quad (4)$$

In order to detect percolation thresholds of the sIPN membranes, proton conductivity the SPEEK/CrPSSA sIPN membranes

was plotted as a function of hydrophilic volume fraction, as shown in Fig. 8. Data for SPEEK and Nafion115 membranes from our previous work [9] were also plotted in Fig. 8 to make a clear comparison. The hydrophilic volume fraction $\phi_+$ is related to relative humidity and could be calculated from the hydrophilic volume (including the volumes of both the $-SO_3H$ groups and water) divided by the volume of the wet membrane. Assuming isotropic expansion in the membranes, $\phi_+$ is given by Equation (5).

$$\phi_+ = \frac{\frac{\rho_{polymer}\overline{V}_{SO_3}}{EW} + \frac{V_{sorption}}{\overline{V}}}{(1+\varepsilon)^3} \quad (5)$$

where $V_{sorption}/\overline{V}$ is the volume of the absorbed water $V_{sorption}$ per unit mass of dry polymer $\overline{V}$, $\varepsilon$ is the linear expansion coefficient obtained from Fig. 6, $\overline{V}_{SO_3}$ is the molar volume of the sulfonic acid group, 40 $cm^3$ $mol^{-1}$. The percolation threshold $(\phi_+)_c$ is identified as the onset hydrophilic volume fraction for a rapid increase in the proton conductivity.

Based on the data shown in Fig. 8, the two critical parameters, percolation thresholds and intrinsic conductivity of different membranes, can be obtained by fitting the conductivity data to Equation (4) with $\alpha = 2$, as listed in Table 3. Intrinsic conductivity is the ability of proton conduction of the ionomers, which depends on the mechanism of proton conduction, acidity and density of the $-SO_3H$ groups in the ionomers [42]. It is seen from Table 3 that the intrinsic conductivities follow the sequence of $\sigma_{0,Nafion} > \sigma_{0,SPEEK/CrPSSA} > \sigma_{0,SPEEK}$. The highest value for Nafion® is mainly related to the highly dissociation of $-SO_3H$ in Nafion®, while higher values for the sIPN membranes than that of the SPEEK membranes are mainly related to the increasing IEC as CrPSSA interpenetrated with SPEEK. Percolation threshold indicates how fast the proton conductivity responses to RH, focusing on the influence of different shape of the conducting domains on the connection ability of the ionic clusters [40,41]. As shown in Fig. 8, Nafion® and SPEEK membranes exhibited the lowest and the highest $(\phi_+)_c$ values, respectively. While the $(\phi_+)_c$ values of SPEEK/CrPSSA sIPN membranes were in between and decreased with the increasing content of CrPSSA in the sIPN membranes. That means ionic clusters in Nafion® are easy to be connected at low hydrophilic volume fraction. This is the reason that the proton conductivity of Nafion® increased rapidly at very low RH, as seen in Fig. 7. Interpenetrating with CrPSSA increased the connection of the ionic clusters in SPEEK membrane, leading to the improvement of proton conductivity at low RH.

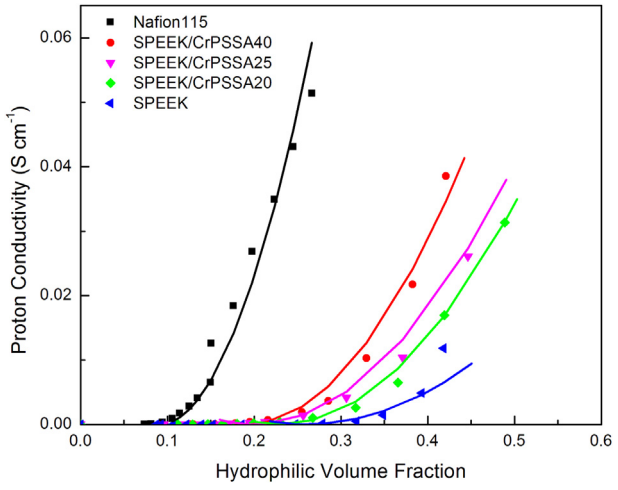


**Fig. 8.** Proton conductivity as a function of hydrophilic volume fraction at 80 °C.

**Table 3**
Proton conductivity parameters for Nafion®, sIPN and SPEEK membranes at 80 °C.

| Ionomers | $\sigma_0$ (S $cm^{-1}$) | $(\phi_+)_c$ | RH at $(\phi_+)_c$ (%) |
|---|---|---|---|
| Nafion115 | 1.9 | 0.09 | 6.8 |
| SPEEK/CrPSSA 40 | 0.65 | 0.18 | 11.5 |
| SPEEK/CrPSSA 25 | 0.45 | 0.20 | 23.2 |
| SPEEK/CrPSSA 20 | 0.47 | 0.23 | 29.6 |
| SPEEK | 0.26 | 0.26 | 53.2 |

Data for Nafion115 and SPEEK membranes were from our previous work [9].

The percolation threshold depends on shapes of the conducting domains [40,41]. For randomly dispersed spherical clusters in a matrix, the percolation threshold for proton conduction occurs at hydrophilic volume fraction of around 0.3. While elongated clusters such as rods or ellipsoids percolate at lower hydrophilic volume fraction of around 0.1 because it is easier for the elongated clusters to build up continuous hydrophilic pathways as compared with spherical shape. Therefore, different values of $(\phi_+)_c$ for SPEEK, SPEEK/CrPSSA sIPN and Nafion® membranes suggest different shapes and connection of ionic clusters in these membranes. The percolation threshold of SPEEK, 0.26, is consistent with spherical ionic clusters. The lower value of $(\phi_+)_c$ for Nafion®, 0.09, indicates elongated ionic clusters. This is also supported by many studies in scattering and microscopy that ionic clusters in Nafion® are more likely rod-like or lamellar shape [43–45]. From Fig. 8, it is also seen that the percolation thresholds of SPEEK/CrPSSA sIPN membranes were in between that of Nafion® and SPEEK membranes, which indicates a different packing structure of $-SO_3H$ groups in the SPEEK/CrPSSA sIPN membranes.

The side chain of Nafion® has the nature of surfactant, in which the hydrophilic polar head $-SO_3H$ connects with the hydrophobic tail perfluoro alky ether (PFAE) side chains. It has been proposed that the side chains of Nafion® tend to form reverse micelles ionic clusters, just like some kinds of surfactants [46]. Due to the comparable projected areal size of the $-SO_3H$ polar head and the PFAE hydrophobic tail, it is likely for Nafion® to form elongated shape ionic clusters [8,47]. And the flexible PFAE side chain provides sufficient flexibility for $-SO_3H$ to pack into the elongated shape. Similar to Nafion®, the benzyl sulfonic acid side chain of PSSA also has the nature of surfactant, which tends to pack into elongated ionic clusters because of the high density of short benzyl sulfonic acid side chains fixed on the hydrophobic main chains. Based on the data observed, we suggest a schematic structural model for proton conduction in the SPEEK/CrPSSA sIPN membranes. As shown in Fig. 9, the crosslinked PSSA networks are interpenetrated with the SPEEK chains. Based on the percolation threshold of SPEEK membrane observed from Fig. 8 ($(\phi_+)_{c,SPEEK} = 0.26$), there are spherical ionic clusters throughout the matrix of SPEEK. In certain regions where the CrPSSA chains are close enough, the $-SO_3H$ would pack into elongated ionic clusters, although the rigidity of the short side chain in CrPSSA restricts the flexibility of $-SO_3H$. As a result, continuous proton conducting pathways establish at lower hydrophilic volume fraction. With the increase of CrPSSA content, there are more elongated packing clusters formed, so that decreases the percolation threshold for proton conduction. The schematic structure model coincides with the percolation threshold investigations in the experimental data (Fig. 8). Additional evidence that supports the combined structural model is the comparable water content (Fig. 5) and a much higher strain of the SPEEK/CrPSSA sIPN and Nafion® membranes (Fig. 6) at low RH as compared with SPEEK membrane. Our previous work shows that packing in spherical clusters may produce more free volume than packing in elongated clusters [9,29]. Therefore, at low RH water absorbed in the free volume around SPEEK clusters does not need to swell the polymer

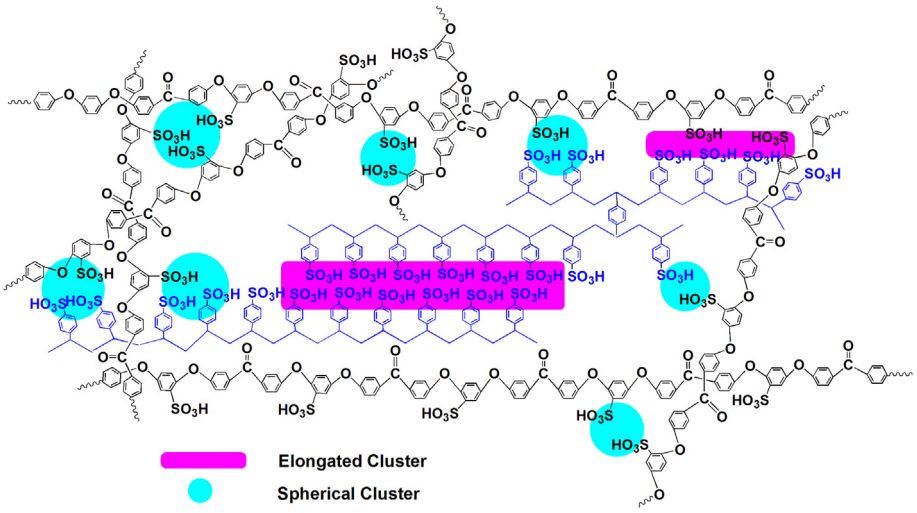


**Fig. 9.** Schematic structure of ionic clusters in the SPEEK/CrPSSA sIPN membranes.

matrix. Swelling of the elongated clusters causes more volume expansion at low RH, and is helpful to build up the interconnection between hydrophilic domains.

According to the structural model proposed in Fig. 9, there are two possible reasons for the increased proton conductivity of the SPEEK/CrPSSA sIPN membranes at low RH as compared with the pristine SPEEK membrane. One reason is the increase of $-SO_3H$ density as CrPSSA content increased, which makes the sulfonic acid groups getting closer and easier to be connected, as indicated by the increased intrinsic conductivity. The other reason is the elongated hydrophilic domains formed in the SPEEK/CrPSSA sIPN membranes, which is easier to percolate at lower RH as compared with spherical hydrophilic domains in SPEEK membrane.

## 4. Conclusion

SPEEK/CrPSSA semi-interpenetrating polymer network (sIPN) membranes were synthesized through the *in-situ* polymerization/crosslinking of sodium 4-styrenesulfonate (NaSS) in the presence of linear SPEEK polymer matrix. Interpenetrating of crosslinked PSSA (CrPSSA) into SPEEK brings the sulfonic acid groups closer and packs them into elongated ionic clusters in the sIPN membranes. As a result, percolation threshold for proton conduction occurs at lower hydrophilic volume fractions as CrPSSA content increased. Proton conductivity of the SPEEK/CrPSSA 40 sIPN membrane starts to increase from RH around 10%, and reaches value of $10^{-3}$ S cm$^{-1}$ at RH 25%, which is close to that of Nafion115, and is 2 orders of magnitude higher than that of the pristine SPEEK membranes ($10^{-5}$ S cm$^{-1}$ at RH 50%). The improved proton conductivity at low relative humidity makes the SPEEK/CrPSSA sIPN membranes attractive as a cost-effective option for PEMFC used as mobile and portable powers.

## Acknowledgments

The authors thank Program for National Science Fund for Distinguished Young Scholars of China (Grant no. 21125628), NSFC (Grant no. 20976027 and 21176044) for the supports of this work. Professor Wu thanks the Chinese Scholarship Council for support to work at Princeton University.

## References

[1] M. Rikukawa, K. Sanui, Prog. Polym. Sci. 25 (2000) 1463–1502.
[2] T.J. Peckham, S. Holdcroft, Adv. Mater. 22 (2010) 4667–4690.
[3] C.H. Park, C.H. Lee, M.D. Guiver, Y.M. Lee, Prog. Polym. Sci. 36 (2011) 1443–1498.
[4] K. Jiao, X. Li, Prog. Energy Combust. Sci. 37 (2011) 221–291.
[5] G. Maier, J.M. Haack, Adv. Polym. Sci. 216 (2008) 1–62.
[6] J. Roziere, D.J. Jones, Annu. Rev. Mater. Res. 33 (2003) 503–555.
[7] A.K. Sahu, G. Selvarani, S.D. Bhat, S. Pitchumani, P. Sridhar, A.K. Shukla, N. Narayanan, A. Banerjee, N. Chandrakumar, J. Membr. Sci. 319 (2008) 298–305.
[8] T. Tamura, R. Takemori, H. Kawakami, J. Power Sources 217 (2012) 135–141.
[9] X. Wu, X. Wang, G. He, J. Benziger, J. Polym. Sci. Part B Polym. Phys. 49 (2011) 1437–1445.
[10] B.P. Tripathi, V.K. Shahi, Prog. Polym. Sci. 36 (2011) 945–979.
[11] D. Xing, G. He, Z. Hou, P. Ming, S. Song, Int. J. Hydrogen Energy 36 (2011) 2177–2183.
[12] L. Du, X. Yan, G. He, X. Wu, Z. Hu, Y. Wang, Int. J. Hydrogen Energy 37 (2012) 1853–1861.
[13] C. Yang, P. Costamagna, S. Srinivasan, J. Benziger, A.B. Bocarsly, J. Power Sources 103 (2001) 1–9.
[14] Y. Yao, Z. Lin, Y. Li, M. Alcoutlabi, H. Hamouda, X. Zhang, Adv. Energy Mater. 1 (2011) 1133–1140.
[15] S. Yi, F. Zhang, W. Li, C. Huang, H. Zhang, M. Pan, J. Membr. Sci. 366 (2011) 349–355.
[16] Q. Li, J.O. Jensen, R.F. Savinell, N.J. Bjerrum, Prog. Polym. Sci. 34 (2009) 449–477.
[17] C. Tsai, C.W. Lin, J. Rick, B. Hwang, J. Power Sources 196 (2011) 5470–5477.
[18] L.E. Karlsson, B. Wesslen, P. Jannasch, Electrochim. Acta 47 (2002) 3269–3275.
[19] Y. Su, Y. Liu, D. Wang, J. Lai, Y. Sun, S. Chyou, W. Lee, J. Membr. Sci. 349 (2010) 244–250.
[20] C.W. Walker, J. Electrochem. Soc. 151 (2004) A1797–A1803.
[21] Z. Dong, S.J. Kennedy, Y. Wu, J. Power Sources 196 (2011) 4886–4904.
[22] C.S. Kim, S.M. Oh, J. Power Sources 109 (2002) 98–104.
[23] L. Chikh, V. Delhorbe, O. Fichet, J. Membr. Sci. 368 (2011) 1–17.
[24] L.H. Sperling, Adv. Chem. Ser. 239 (1994) 3–38.
[25] Y.S. Lipatov, T.T. Alekseeva, Adv. Polym. Sci. 208 (2007) 1–227.
[26] X. Wu, G. He, S. Gu, Z. Hu, P. Yao, J. Membr. Sci. 295 (2007) 80–87.
[27] X. Wu, G. He, S. Gu, Z. Hu, X. Yan, Chem. Eng. J. 156 (2010) 578–581.
[28] X. Wu, G. He, L. Gao, S. Gu, Z. Hu, P. Yao, Chin. Chem. Lett. 17 (2006) 965–968.
[29] Q. Zhao, P. Majsztrik, J. Benziger, J. Phys. Chem. B 115 (2011) 2717–2727.
[30] Q. Zhao, N. Carro, H.Y. Ryu, J. Benziger, Polymer 53 (2012) 1267–1276.
[31] P.W. Majsztrik, A.B. Bocarsly, J. Benziger, Macromolecules 41 (2008) 9849–9862.
[32] C. Yang, S. Srinivasan, A.B. Bocarsly, S. Tulyani, J. Benziger, J. Membr. Sci. 237 (2004) 145–161.
[33] W.H. Choi, W.H. Jo, J. Power Sources 188 (2009) 127–131.
[34] V.D. Noto, M. Piga, G.A. Giffin, G. Pace, J. Membr. Sci. 390–391 (2012) 58–67.
[35] S.J. Peighambardoust, S. Rowshanzamir, M.G. Hosseini, M. Yazdanpour, Int. J. Hydrogen Energy 36 (2011) 10940–10957.
[36] C. Yang, Int. J. Hydrogen Energy 36 (2011) 4419–4431.
[37] H.L. Frisch, Prog. Org. Coat. 27 (1996) 67–72.
[38] W. Vielstich, H. Yokokawa, H.A. Gasteiger (Eds.), Handbook of Fuel Cells: Advances in Electrocatalysis, Materials, Diagnostics and Durability, vols. 5 and 6, John Wiley & Sons, Chichester, 2009, pp. 345–358.
[39] T.D. Gierke, G.E. Munn, F.C. Wilson, J. Polym. Sci. Part B Polym. Phys. 19 (1981) 1687–1704.
[40] D.S. Aharony, An Introduction to Percolation Theory, Taylor and Francis, London, 1992.

[41] S. Torquato, Random Heterogeneous Materials. Microstructure and Macroscopic Properties, Springer, New York, 2002.
[42] W.Y. Hsu, J.R. Barkley, P. Meakin, Macromolecules 13 (1980) 198–200.
[43] K. Schmidt-Rohr, Q. Chen, Nat. Mater. 7 (2008) 75–83.
[44] X. Kong, K. Schmidt-Rohr, Polymer 52 (2011) 1971–1974.
[45] L. Rubatat, G. Gebel, O. Diat, Macromolecules 37 (2004) 7772–7783.
[46] D.B. Spry, A. Goun, K. Glusac, D.E. Moilanen, M.D. Fayer, J. Am. Chem. Soc. 129 (2007) 8122–8130.
[47] K. Esumi, U. Minoru, Structure–performance Relationships in Surfactants, Marcel Dekker, New York, 2003.